ARTICLES

Transient Absorption and Resonance Raman Investigations on the Axial Ligand Photodissociation of Halochromium(III) Tetraphenylporphyrin

Sae Chae Jeoung and Dongho Kim*

National Creative Research Initiatives Center for Ultrafast Optical Characteristics Control and Spectroscopy Laboratory, Korea Research Institute of Standards and Science, Taejon 305-600, Korea

Dae Won Cho

Department of Chemistry, Seonam University, Namwon, Chonbuk 590-711, Korea

Minjoong Yoon

Department of Chemistry, Chungnam National University, Taejon 305-764, Korea

Received: June 18, 1999; In Final Form: December 8, 1999

The axial ligand photodissociation processes of halochromium(III) tetraphenylporphyrin ($XCr^{III}TPP$, X = Cl, Br) have been investigated in noncoordinating and coordinating solvents by transient Raman and absorption spectroscopic techniques. In noncoordinating solvents such as benzene, the upshift of the ν_2 and ν_4 bands and the disappearance of Cr—X stretching mode in the transient Raman spectra demonstrate the core size reduction of the porphyrin macrocycle accompanied by the photodissociation of axial halogen ligand atoms in the excited state. In coordinating solvents such as tetrahydrofuran (THF), where the solvent molecule is already attached to $XCr^{III}TPP$ as an axial ligand to form $XCr^{III}TPP(THF)$, the transient spectroscopic data indicate that the axial halogen ligand atoms photodissociate to form the five-coordinate $Cr^{III}TPP(THF)$ on photoexcitation. The temporal evolutions of photoinduced absorption and bleaching signals of $XCr^{III}TPP$ in benzene exhibit biphasic decay profiles with time constants of 1 and 20 ms. The shorter decay is likely due to the four-coordinate photoexcited $Cr^{III}TPP^*$ species, and the relatively slow decay component seems to be the recombination process returning to the original five-coordinate $XCr^{III}TPP$ species. On the other hand, a significant reduction in the lifetime of photoexcited $ClCr^{III}TPP$ in THF was observed as compared with that in benzene. This behavior seems to be caused by the excited five-coordinate $Cr^{III}TPP(THF)^*$ species, which decays rapidly with a time constant of 632 ps due to the participation of low-energy states in the deactivation process below the normally emissive tripmultiplet (π,π^*) states. The electronic nature of the lowest excited state of the five-coordinate $Cr^{III}TPP(THF)^*$ species is suggested to possess (π,d_π) charge transfer character based on the comparison of transient Raman and absorption spectral features with those of other paramagnetic metalloporphyrins. We explain the axial ligand photodissociation processes in terms of the electron density change in metal d orbitals, which is particularly sensitive to the interaction with σ-donor axial ligands.

1. Introduction

The photochemical properties of metalloporphyrins have received much attention because of their biological implications and use in a variety of photocatalytic reactions.[1−3] In particular, the axial ligand photodissociation or photoassociation of metalloporphyrins has been of considerable interest because the investigation of this phenomena can provide further information related to the biological functions of axial ligands in heme proteins.[4−8] It has been relatively well established that the biological function of heme proteins is significantly influenced by the axial ligation of the heme moiety. The axial ligand strongly affects the electronic structure and the reactivity of metalloporphyrins in both ground and excited states.[9] As a continuing effort to develop our understanding of the porphyrin structural change in the excited states induced by the axial ligand, we have explored the photophysics as well as the photochemistry of the photoinduced ligand dissociation and association processes for Cr^{III} porphyrins. The motivation for this approach coincides well with the fact that the axial ligand in Cr^{III} porphyrins is known to be anomalously labile despite of the high ligand affinity of Cr^{III} porphyrins.[10−12]

Recently, there have been several studies on the photophysical properties of Cr^{III} porphyrins. Hoshino et al.[12−15] carried out laser flash photolysis of $ClCr^{III}TPP(L)$ (L = sixth axial ligand) in various solvents to elucidate the photodissociation mechanism of the axial ligand. They proposed that the $^4S_1(\pi,\pi^*)$ excited state acts as the main route of photodissociation process and its yield markedly depends on the nature of the axial ligand. As for the axial ligand exchange reaction, Summerville et al.[11] suggested that the alteration of the sixth ligand induces structural

* To whom correspondence should be addressed.

10.1021/jp9920287 CCC: $19.00
Published on Web 05/05/2000

changes in metalloporphyrins, especially the planarity of the central Cr^{III} metal relative to the porphyrin macrocycle plane. It is known that a variety of photophysical and photochemical properties of Cr^{III} porphyrins arise from intramolecular charge transfer (CT) processes.[16]

Cr^{III} metal has a d^3 electronic configuration with half-filled d_{xy}, d_{yz}, and d_{xz} orbitals and empty $d_{x^2-y^2}$ and d_{z^2} orbitals. As a result of coupling between the porphyrin and metal electronic transitions, the ground and singlet excited $^1(\pi,\pi^*)$ states become quartet $^4S(\pi,\pi^*)$, whereas the excited triplet state $^3(\pi,\pi^*)$ is split into tripdoublet $^2T(\pi,\pi^*)$, tripquartet $^4T(\pi,\pi^*)$, and tripsextet $^6T(\pi,\pi^*)$ states. In addition to these (π,π^*) transitions, the intramolecular CT transitions between porphyrin π- and metal d-orbitals and the (d,d) transitions among metal d-orbitals are also possible. Cr^{III} porphyrins have been the subject of numerous investigations because of their anomalous luminescence properties[13,16,17] caused by the coupling of unpaired metal d electrons with the porphyrin ring (π,π^*) transitions. Gouterman et al.[17] reported that the two luminescent bands from $ClCr^{III}TPP$ in the 800−850-nm region originate from tripquartet $^4T(\pi,\pi^*)$ and tripsextet $^6T(\pi,\pi^*)$ states formed by the interaction between Cr^{III} metal and porphyrin (π,π^*) excited triplet state. A recent investigation on the luminescent properties of Cr^{III} porphyrins showed that the lifetime of the photoexcited state is relatively short (∼295 ps in ethanol)[16] and depends strongly on the solvents employed. A substantial decrease in the lifetimes of photoexcited $ClCr^{III}TPP$ compared with other diamagnetic matalloporphyrins was ascribed to the possible existence of a low-energy (d,d) or CT state that acts as a quenching state of the luminescent tripmultiplet (π,π^*) states. Meanwhile, $ClCr^{III}$-TPP(py) in acetone exhibits an excited-state absorption peak at ∼480 nm with a lifetime of 118 ns at room temperature,[15] indicating that the solvents employed play an important role in deactivation routes of photoexcited Cr^{III} porphyrins. However, there is little information on the structural changes and photophysical properties of Cr^{III} porphyrins induced by the photodissociation of the axial ligand.

Therefore, in this work, transient Raman and transient absorption spectroscopic studies were carried out to obtain further insight into the photodissociation processes of the axial ligand and the structural changes of porphyrin macrocycle in the excited states. In this investigation, we found that the axial halogen atoms of Cr^{III} porphyrins photodissociate in the excited states.

2. Experimental Section

$ClCr^{III}TPP$ and $BrCr^{III}TPP$ were purchased from Porphyrin Products (Logan, UT) and purified by aluminum column chromatography prior to usage. Benzene and tetrahydrofuran (THF) were used after the literature purification. The porphyrin concentration was $\sim10^{-5}$ M. All the transient Raman experiments were performed by flowing the sample solution through a glass capillary (0.8-mm i.d.) at a rate sufficient enough to ensure that each laser pulse encounters a fresh volume of the sample unless specified.

The transient RR spectra were obtained by using 416 nm pulses, generated by the hydrogen Raman shifting of the third (355 nm) harmonics from a nanosecond Q-switched Nd:YAG laser. The Raman spectra were collected with an HR 640 spectrograph (Jobin-Yvon), a gated intensified photodiode array detector (Princeton Instruments IRY700), and a pulse generator (Princeton Instruments FG100).[18]

Steady-state photoinduced absorption spectra were recorded with the 442 nm line of a HeCd cw laser as a pump beam and a tungsten-halogen lamp as a probe beam. The pump beam was modulated by a fast homemade shutter with a typical closing time of <1 ms. The absorbance difference signal was passed through a monochromator and measured with a gated photon counter. A typical setup for nanosecond flash photolysis was composed of a Q-switched Nd:YAG laser, a boxcar averager, and a 500 MHz digital oscilloscope. Ground-state absorption spectra were recorded on a Varian ultraviolet−visible (UV-vis) spectrophotometer (Cary 5E).

The dual-beam femtosecond time-resolved transient absorption spectrometer consisted of a self-mode-locked femtosecond Ti:sapphire laser (Spectra Physics, Tsunami), a Ti:sapphire regenerative amplifier (Quantronix) pumped by a Q-switched Nd:YLF laser, a pulse stretcher/compressor, and an optical detection system.[19] The final laser pulses had a pulse width of ∼200 fs and an average power of 300 mW. The pump pulses at 400 nm were generated by frequency doubling in a β-BBO crystal. The residual fundamental beam was focused onto a quartz window to generate a white light continuum, which was again split into two parts: one for probing the transient and the other for the reference. The time delay between pump and probe pulses was adjusted by a variable optical delay line. The white light continuum pulses after the samples were dispersed by an 18-cm focal length spectrograph (Scientific Instruments) and then detected by a dual 512 channel photodiode array detector (Princeton Instruments). The intensity of the white light of each 512-channel photodiode array was processed to calculate the absorption difference spectrum at the desired time delay. For the precise measurements of temporal profiles of transient absorption signals, the monitoring wavelength was selected by putting an appropriate interference filter [full width at half-maximum (fwhm) = 10 nm], and then split into two parts (probe and reference). By chopping the pump pulses at 40 Hz, the modulated probe as well as the reference pulses were detected by two separate photodiodes. The output current was amplified by a homemade fast preamplifier, and then the resultant voltage of the probe pulses was normalized by a boxcar averager with a pulse-to-pulse configuration. The resultant signal modulated by a chopper was measured by a lock-in amplifier and then fed into a personal computer for further processing.

3. Results

Figure 1 shows the transient Raman spectra of $XCr^{III}TPP$ (X = Cl, Br) in benzene recorded by nanosecond pulse excitation at 416 nm. The Raman spectrum was strongly dependent on the laser power; the intense nanosecond laser pulse at 416 nm populates the tripmultiplet (π,π^*) states of Cr^{III} porphyrins and simultaneously probes the tripmultiplet (π,π^*) states Raman spectrum via resonance Raman scattering. The ground-state Raman spectrum of $ClCr^{III}TPP$ was obtained by very low-power laser pulse excitation [Figure 1A(a)]; ν_2 mode at 1550 cm^{-1}, ν_4 mode at 1363 cm^{-1}, ν_1 mode at 1234 cm^{-1}, and ν_8 mode at 392 cm^{-1}. No change in the frequencies of these modes was found on substitution of the axial ligand Cl to Br ion (Table 1). The axial ligand modes at 345 cm^{-1} for $ClCr^{III}TPP$ (Cr—Cl stretching) and at 320 cm^{-1} for $BrCr^{III}TPP$ (Cr—Br stretching) were also clearly observed [see Figures 1A(a) and 1B(a)]. To obtain the Raman spectrum contributed purely by the excited tripmultiplet (π,π^*) states of $XCr^{III}TPP$ [Figure 1A(c)], the ground-state Raman spectral features of $XCr^{III}TPP$ [Figure 1A(a)] were subtracted from the Raman spectrum acquired by high-power photoexcitation [Figure 1A(b)] using a proper subtraction factor to eliminate any contribution from the ground-state complex. Comparing Figure 1A(c) with the spectrum in

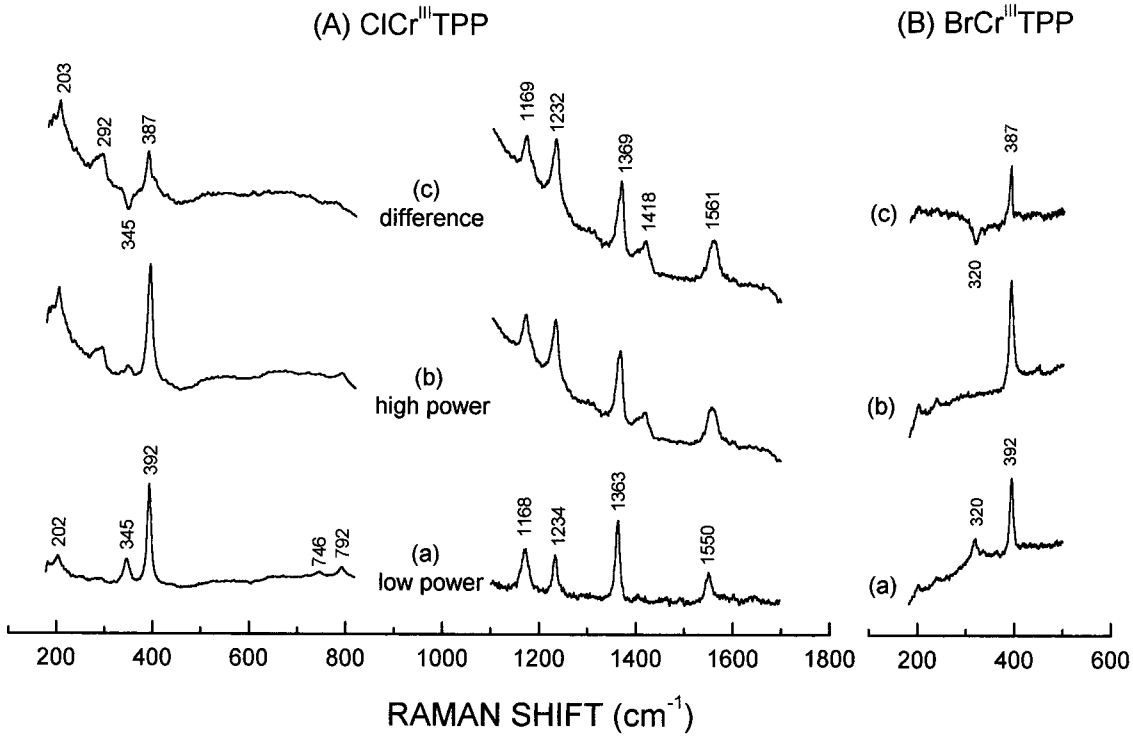

Figure 1. Nanosecond transient resonance Raman spectra of (A) ClCr^{III}TPP and (B) BrCr^{III}TPP in benzene with both pump and probe pulses at 416 nm: (a) the low-power (~0.01 mJ/pulse), (b) the high power (~0.2 mJ/pulse), and (c) the difference spectra (b − a) with a proper scaling factor. The solution was flowed so a fresh sample was exposed to every laser pulse.

TABLE 1: Assignment of Vibrational Modes of Cr^{III} Porphyrin in Various Solvents

mode	symmetry	assignment	XCr^{III}TPP	Cr^{III}TPP*	XCr^{III}TPP(L)	Cr^{III}TPP(L)*
ν_2	a_{1g}	$\nu(C_\beta{-}C_\beta),\nu(C_\beta{-}H)$	1550	1561	1562	1540
ν_3	a_{1g}	$\nu(C_\alpha{-}C_m)$			1420	
ν_4	a_{1g}	$\nu(C_\alpha{-}N),\delta(C_\beta{-}H)$	1363	1369	1363	1352
ν_1	a_{1g}	$\beta(C_m{-}ph)$	1234	1232	1233	1226
					636	636
ν_8	a_{1g}	$\nu(Cr{-}N)$	392	387	392	385
γ_2	a_{1u}	pyr swivel				335
γ_6	a_{2u}	pyr tilt		292	292	
Cr—Cl		Cr—Cl	345		345	
Cr—Br		Cr—Br	320		318	
γ_7	a_{2u}	$\gamma(C_\alpha{-}C_m)$				263
δ_{10}	a_{1g}	$\nu(C_m{-}ph)$	202	204	204	201

Figure 1A(a), it is noteworthy that the ν_2 and ν_4 bands were shifted to 1561 and 1369 cm^{-1}, respectively. Because the other modes, such as ν_8 mode, exhibit a frequency shift in the excited state, the negative feature for Cr—X (X = Cl, Br) stretching modes at 345 and 320 cm^{-1} upon photoexcitation, as shown in the difference spectrum of Figure 1(c), is indicative of the loss of halogen axial ligand.

Because Cr^{III} metal has an available σ-bonding site for the sixth axial ligation, the axial ligand affinity of Cr^{III} porphyrin is known to be higher than other metalloporphyrin complexes.[11] Thus, in THF solution of Cr^{III} porphyrin, the solvent molecule acts as a σ-donor to form a six-coordinate Cr^{III} porphyrin, XCr^{III}-TPP(THF), in the ground state. The ground-state Raman spectrum of ClCr^{III}TPP(THF) could be obtained by very-low-power photoexcitation [Figure 2A(a)]; ν_4 mode at 1363 cm^{-1}, ν_1 mode at 1233 cm^{-1}, ν_8 mode at 392 cm^{-1}, and Cr—Cl stretching mode at 345 cm^{-1} (Table 1). The Cr—Br stretching band was observed at 318 cm^{-1} as shown in Figure 2B(a). It is interesting to note that the ν_2 mode was observed at 1550 cm^{-1} with an overlap of another peak at 1562 cm^{-1}, an indication of the coexistence of two different molecular species. The ν_2 mode at 1550 cm^{-1} is likely to originate from the five-coordinate complex, whereas the one at 1562 cm^{-1} probably arises from the six-coordinate ClCr^{III}TPP(THF) species. The five-coordinate adduct observed in this Raman spectrum is believed to be the mixture of ClCr^{III}TPP and Cr^{III}TPP(THF). This argument can be further supported by the relative Raman intensity ratio decrease between X—Cr^{III} stretching mode and ν_8 mode at 392 cm^{-1} in THF [Figures 2A(a) and 2B(a)] as compared with that in benzene [Figures 1A(a) and 1B(a)], indicating that the axial halogen atoms are partially replaced by THF solvent molecules to form Cr^{III}TPP(THF) species. We recorded the transient resonance Raman spectrum of XCr^{III}TPP(THF) in THF as shown in Figures 2A(c) and 2B(c) under high-power laser pulse illumination at 416 nm. In comparison with the spectrum of Figure 2A(a), an apparent increase in the intensities of some Raman peaks becomes manifest; ν_2 mode at 1540 cm^{-1}, ν_4 mode at 1352 cm^{-1}, ν_1 mode at 1226 cm^{-1}, and ν_8 mode at 385 cm^{-1}. Furthermore, the ν_2 and ν_4 bands shift to low frequency, and the Raman peaks corresponding to Cr—Cl and Cr—Br stretching modes are diminished. Two Raman bleaching bands at 1562 and 1420 cm^{-1} observed in the difference spectrum in Figure 2(c) demonstrate a complete conversion of XCr^{III}TPP(THF) species to the five-coordinate Cr^{III}TPP(THF) on photoexcitation.

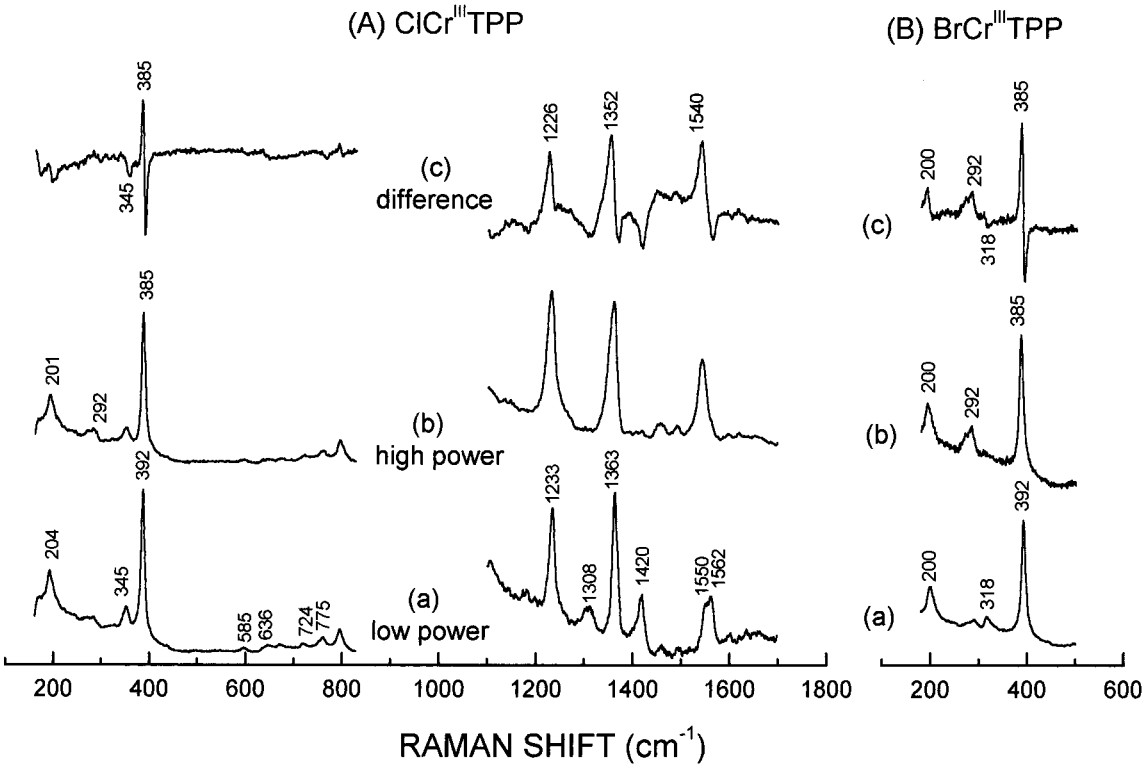

Figure 2. Nanosecond transient resonance Raman spectra of (A) ClCr^{III}TPP(THF) and (B) BrCr^{III}TPP(THF) in THF with both pump and probe pulses at 416 nm: (a) the low-power (~0.01 mJ/pulse), (b) the high power (~0.2 mJ/pulse), and (c) the difference spectra (b − a) with a proper scaling factor. The solution was flowed so a fresh sample was exposed to every laser pulse.

Meanwhile, the Raman peak at 1562 cm^{-1} of the six-coordinate ClCr^{III}TPP(THF) species is large compared with that at 1550 cm^{-1} of the five-coordinate Cr^{III}TPPCl species at low power excitation. The relative Raman intensity at 1550 cm^{-1} increased as the laser power increased (data not shown). In parallel with this result, the relative Raman intensities of the ν_1 and ν_4 modes at 1234 and 1363 cm^{-1} increased without frequency shift with an increase in laser power. The increased peaks were believed to originate from the five-coordinate Cr^{III}TPP(THF) species as already described. Furthermore, the ν_1, ν_2, and ν_8 modes of the five-coordinate species in benzene and six-coordinate species in THF were observed incidentally at the same frequencies. Thus, we suggest that the frequencies of ν_1, ν_2, and ν_8 modes of the five-coordinate Cr^{III}TPP(THF) and six-coordinate ClCr^{III}-TPPP(THF) species are similar and, consequently, not resolved in our experiment.

We recorded the Raman spectra of XCr^{III}TPP in THF after letting the solution stand at room temperature for several days [Figures 3A(a) and 3B(a)]. Interestingly, we could not observe the X—Cr^{III} stretching modes and the ν_2 mode at 1562 cm^{-1} contributed by the six-coordinate XCr^{III}TPP(THF) species in the ground state. These experimental observations indicate that the axial ligand halogen atoms gradually dissociate in the ground state. This result is not so surprising because Cr^{III} porphyrin complexes are known to exchange the axial ligands, rather easily, particularly with alcohols, water, or halide ions.[17] The transient Raman spectra of this solution exhibit the ν_2 mode at 1540 cm^{-1} and the ν_4 mode at 1352 cm^{-1} in the high-frequency region, corresponding to the excited state of the five-coordinate complex Cr^{III}TPP(THF)* [Figure 3(c)]. We observed similar Raman spectral changes for Cr^{III} porphyrin in THF when the sample was not flowed (data not shown). On the contrary, as the sample was flowed to ensure the exposure of the fresh volume to the incoming low-power laser pulses, the Raman peak at 1420 cm^{-1} and the shoulder at 1562 cm^{-1} were clearly enhanced. But these modes vanish in the nanosecond pulse excitation Raman spectra by increasing the laser power while keeping the other experimental conditions the same [Figure 2A(b)]. These experimental results suggest that the incoming photon facilitates the axial ligand dissociation of XCr^{III}TPP in THF. All the experimental observations can be summarized in the following scheme:

In noncoordianting solvents (benzene, CH_2Cl_2, methylcyclohexane)

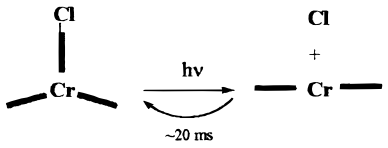

In coordinating solvents (THF, pyridine)

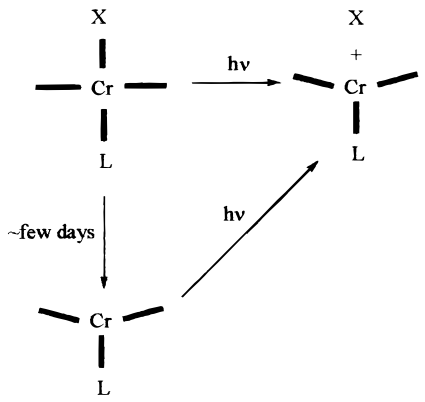

where L = THF or pyridine.

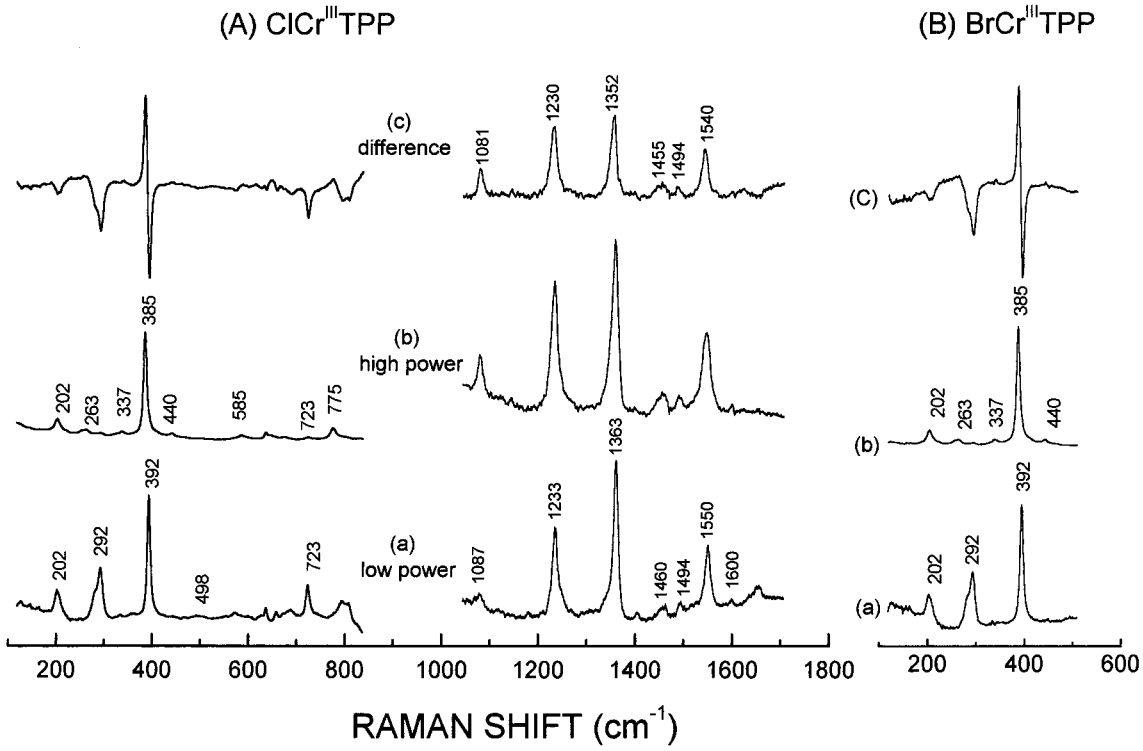

Figure 3. Nanosecond transient resonance Raman spectra of (A) ClCr^{III}TPP and (B) BrCr^{III}TPP in THF with both pump and probe pulses at 416 nm: (a) the low-power (~0.01 mJ/pulse), (b) the high power (~0.2 mJ/pulse), and (c) the difference spectra (b − a) with a proper scaling factor. The sample solutions were allowed to stand at room temperature for several days. The axial ligand halogen atoms are replaced by THF even in the ground state. The solution was flowed so a fresh sample was exposed to every laser pulse.

The ground-state absorption spectra of ClCr^{III}TPP in THF and benzene exhibit absorption maxima at 446 and 451 nm, respectively, in the Soret band region, as shown in Figure 4A. These absorption spectral features are in accordance with those reported in a noncoordinating solvent like dichloromethane,[15] and in a coordinating solvent, like THF.[11] This agreement indicates that benzene does not affect the axial ligand nature and the ground-state electronic structure of Cr^{III} porphyrin, whereas THF solvent acts as a σ-donor to form a six-coordinate Cr^{III} porphyrin, ClCr^{III}TPP(THF), in the ground state. To investigate the dynamics of the excited four-coordinate adduct in benzene, we measured the steady-state photoinduced absorption spectra with the 442 nm line of a cw HeCd laser. The resultant spectra exhibit interesting derivative-like features with the photoinduced absorption maximum at 446 nm and the bleaching peak at 453 nm (Figure 4B). A series of these spectra exhibit only one isosbestic point on increasing the laser power, suggesting that two different chemical species participate in the photoinduced reaction. These results also led us to conclude that the axial ligand chlorine transiently detaches from Cr^{III} metal to form a four-coordinate adduct. We measured the temporal profiles of photoinduced absorption and bleaching signals at 446 and 453 nm, respectively, with photoexcitation at 442 nm using a cw HeCd laser (Figure 4C). The decay profiles of both photoinduced absorption and bleaching exhibit single-exponential decay, with time constants of 19.0 and 20.9 ms, respectively. The photoprocess of Cr^{III} porphyrins being observed in benzene is the photodissociation of the chloride ion, which results in a four-coordinate complex. Benzene is known to be an inert solvent for the axial ligation. Thus, because the concentration of chloride ion is very low relative to the solvent (6 orders of magnitude lower), the long-time scales associated with the recovery of the original five-coordinate ClCr^{III}TPP species are consistent with dilute species being present, rather than unfavorable complexation with omnipresent benzene solvent molecules.

To draw definitive conclusions regarding these peculiar phenomena, a nanosecond laser flash photolysis experiment was also performed. The transient absorption spectra at various time delays and their decay profiles at 446 and 453 nm using ~5 ns laser pulse excitation at 435 nm are shown in Figures 5A and 5B, respectively. In addition to the similarities between the transient absorption spectra in Figures 4B and 5A, we observed an additional fast component with time constants of ~1 ms in the temporal evolutions of photoinduced absorption and bleaching signals. Because the time constant of the fast decay component is close to that of photoexcited ClCr^{III}TPP in noncoordinating solvent such as CH_2Cl_2, the fast transient species is likely to be the excited state of ClCr^{III}TPP.[15] Furthermore, the complete recovery of the bleaching band at ~453 nm with a gradual shift to shorter wavelength with an increase in time delay (see Figure 5A) indicates that the transient four-coordinate adduct, Cr^{III}TPP*, returns to the original five-coordinate species with a time constant of ~20 ms.

The steady-state photoinduced absorption changes of ClCr^{III}-TPP in THF were recorded by the 442 nm line from a cw HeCd laser (Figure 6A). The difference absorption spectra exhibit a bleaching peak at 446 nm and a positive but weak one at 458 nm. On photoexcitation, the axial ligand chlorine of ClCr^{III}-TPP(THF) photodissociates, giving rise to an absorption increase at 458 nm to the red side of the bleaching band. We were able to observe the transient Raman bands of photoexcited Cr^{III}TPP-(THF)* species only by the one-color nanosecond transient Raman experiment and not by the two-color nanosecond pump/probe transient Raman experiment at various time delays. Similarly, no transient absorption signal was detected with photoexcitation by nanosecond pulses at 416 nm. These experimental observations indicate that the lifetime of photoexcited Cr^{III}TPP(THF)* adduct is shorter than the nanosecond time scale. Thus, by using ~200 fs laser pulses at 400 nm, we were able to record the transient absorption spectra of ClCr^{III}-

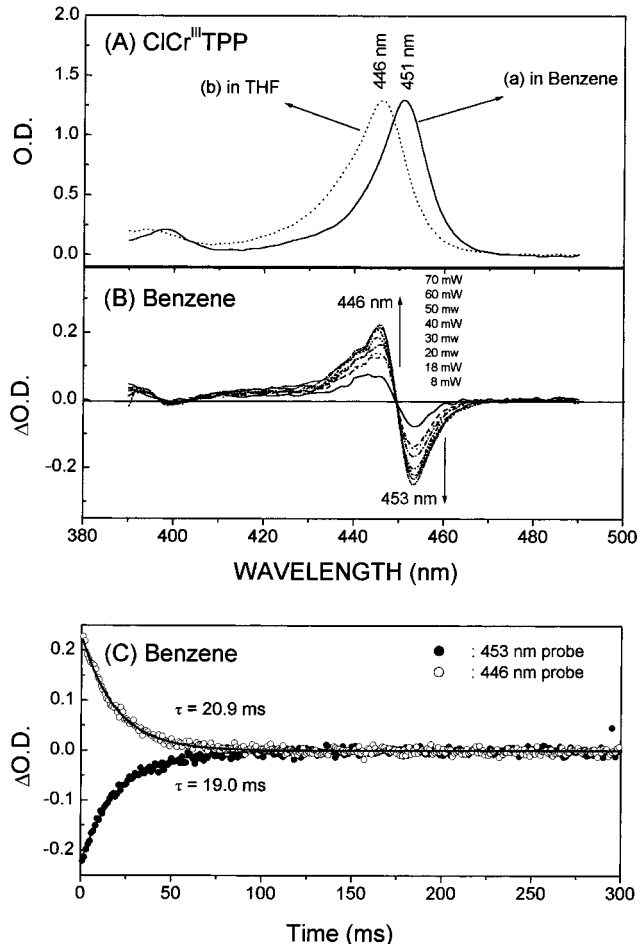

Figure 4. (A) Optical absorption and (B) steady-state photoinduced absorption spectra for the degassed solution of ClCr^{III}TPP. Steady-state photoinduced absorption spectra were recorded at room temperature by pumping at 442 nm. (C) Decay profiles of photoinduced absorption at 446 nm (open circles) and absorption bleaching at 453 nm (closed circles) for the degassed solution of ClCr^{III}TPP in benzene. The average power of pump beam at 442 nm is ~70 mW.

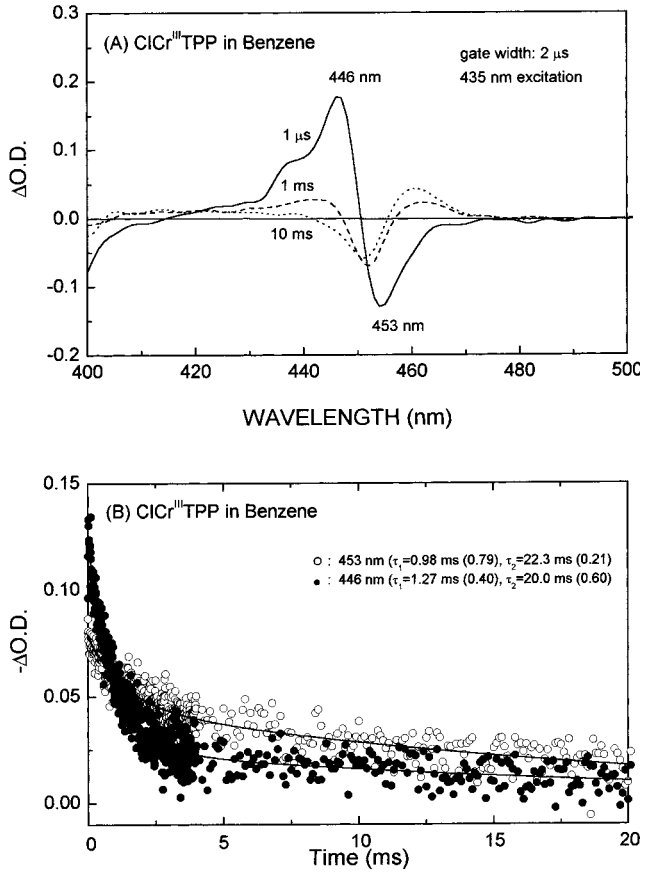

Figure 5. (A) Transient absorption spectrum after excitation at 435 nm in various time delays and (B) its decay profiles recorded at 446 (closed circles) and 453 nm (open circles) for ClCr^{III}TPP in benzene.

TPP in THF (Figure 6B). The overall transient absorption spectra exhibit broad and featureless absorption with a slight dip due to the Q-band bleaching, which returns to the ground state with a time constant of 632 ps (Figure 6C). Taking into account that THF solvent molecules can bind to the central Cr^{III} metal and the axial ligand chlorine is labile, the transient absorption spectra recorded by femtosecond optical pulses are attributable to the excited-state, five-coordinate adduct Cr^{III}TPP(THF)*.

4. Discussion

Structural Changes of Cr^{III} Porphyrins in the Excited States. It is known that the high-frequency Raman modes of metalloporphyrins have a strong correlation with the porphyrin geometry as well as its electronic structure. The primary focus of our discussion is the totally symmetric modes, ν_2 and ν_4 modes, whose frequencies are known to be strongly dependent on the core size of the porphyrin marcrocycle.[20] On the basis of theoretical molecular orbital (MO) calculations on metalloporphyrins[21] and free-base porphyrins,[22] the a_{1u} and a_{2u} orbitals are antibonding and bonding with respect to C_β—C_β bond, respectively, and the e_g orbital is slightly antibonding. Therefore, ($a_{1u}e_g$) and ($a_{2u}e_g$) configurations in the excited state are expected to yield stronger and weaker C_β—C_β bonds, respectively, than those in the ground state. The triplet states of metallo-TPPs have ^{3}($a_{2u}e_g$) electronic configuration,[23,24] reflecting the expected reduction in C_β—C_β bond order on extracting an electron from the a_{2u} orbital and placing it in the e_g orbital. Therefore, the ν_2 mode (C_β—C_β stretching) is expected to exhibit a downshift in the excited triplet state compared with the ground state. However, contrary to this expectation, our results in benzene show the upshift of ν_2 and ν_4 modes implying that the structural changes of porphyrin macrocycle in the excited state are not affected simply by the change of electronic configurations.

Zwaans et al.[25] recently reported the theoretical prediction that Cr^{III} metal of the five-coordinate adduct does not lie in the porphyrin ring plane because the axial halogen atom pulls the central metal out of the porphyrin plane. It is likely that Cr^{III} metal tends to move into the porphyrin plane when the sixth ligand binds to the central metal at the opposite site from the halogen atom. This argument is supported by the electron spin resonance (ESR) data on ClCr^{III}TPP(THF)[11] and X-ray structure analysis of ClCr^{III}TPP(imidazole),[26] demonstrating the position of Cr^{III} metal lying in the porphyrin ring plane. Thus, two molecular species of Cr^{III} porphyrin in benzene that yield different frequencies in the ν_2 Raman mode are most likely to arise from the difference in their core sizes. As the axial ligand halogen atoms dissociate from the central metal to form the four-coordinate adduct, Cr^{III} metal tends to move into the porphyrin ring plane. As a result, the core size of the porphyrin macrocycle decreases, which in turn results in an increase in the frequencies of the totally symmetric ν_2 and ν_4 modes. This prediction describes well the direction of the Raman frequency shift for the five- and six-coordinate Cr^{III} porphyrins, as listed in Table 1. The relationship between the porphyrin core size and the frequencies of some high-frequency Raman modes has usually been described by the expression[20] $\nu_i = K(A - d_i)$, where

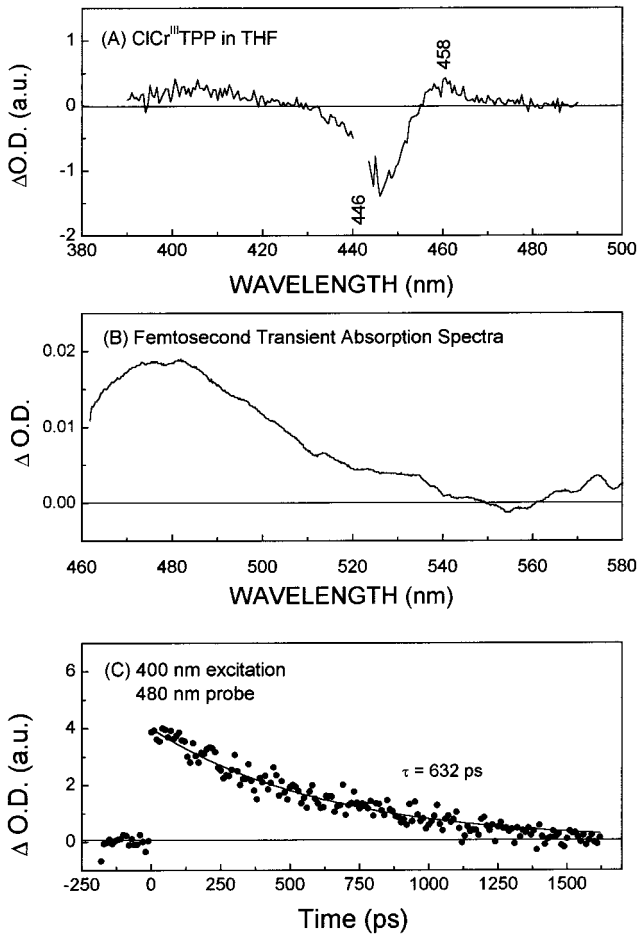

Figure 6. (A) Steady-state photoinduced absorption spectrum, (B) the transient absorption spectrum at zero time delay, and (C) its decay profiles measured at 480 nm for ClCr^{III}TPP solution in THF. The average power of the pump pulse at 400 nm is ~8 mW, with a 1 kHz repetition rate.

K and *A* are characteristic parameters of porphyrin macrocycle. The core size differences [$\Delta\nu = K(d_{nonpl} - d_{pl})$] between nonplanar five-coordinate XCr^{III}TPP and planar four-coordinate Cr^{III}TPP* were estimated to be 0.035 and 0.043 Å by employing $K = 312.5$ and 138.9 cm^{-1}/Å, respectively, and the frequency upshift of ν_2 and ν_4 modes ($\Delta\nu$) for XCr^{III}TPP in benzene (Figure 1). Similarly, in the case of XCr^{III}TPP in THF, the core size difference between five-coordinate XCr^{III}TPP and planar six-coordinate XCr^{III}TPP(THF) adducts [$(\Delta\nu = K(d_{nonpl} - d_{pl})$] was calculated to be 0.038 Å [Figure 2A(a)] using the upshift of the ν_2 mode ($\Delta\nu$). As previously reported for the Cu^{II} porphyrins from our laboratory,[27] the porphyrin core size of paramagnetic Cu^{II}TPP markedly changes by ~0.065 Å through the formation of a five-coordinate complex when an axial ligand is added to the Cu^{II} metal of the four-coordinate porphyrin. The Cu^{II} metal in the five-coordinate complex was suggested to move out-of-plane by ~0.5 Å.[28] It might be pointed out that the core size difference between the two paramagnetic porphyrins estimated from the Raman frequency shift has a linear correlation with the movement of central metal from the porphyrin ring plane.

Electronic Nature of the Lowest Excited State of Cr^{III} Porphyrins in Coordinating Solvents. Numerous previous investigations revealed that the binding of the fifth-ligand to the photoexcited Cu^{II} porphyrins results in a drastic decrease in the lifetime of this species by lowering the energy of the quenching state, such as (π,d) CT or (d,d) state below the normally emissive tripmultiplet (π,π^*) states.[27,28] In such cases, the fifth ligands are known to be σ-donor solvents, such as THF, dioxane, water, pyridine, and piperidine.[19,24] The transient Raman spectroscopic data of this exciplex also show that the downshift of ν_2 and ν_4 modes by ~20 cm^{-1} in the exciplex formation is accompanied by movement of Cu^{II} metal out of the porphyrin ring plane. Thus, the relatively large shift of the ν_2 and ν_4 modes by ~20 cm^{-1} in the exciplex formation was interpreted in terms of both metal out-of-plane geometry and participation of the low-energy quenching state with the electronic nature of (π,d) CT or (d,d) transition. The iterative extended Huckel calculation[17] predicts that a vacant d_{z^2} and half-filled d_{xy}, d_{yz}, and d_{xz} orbitals of Cr^{III} metal are located between LUMO $e_g(\pi^*)$ and HOMO $a_{2u}(\pi)$ orbitals of porphyrin ring, whereas an empty $d_{x^2-y^2}$ orbital lies well above the $e_g(\pi^*)$ orbital (Figure 7A). Based on this calculation, it is likely that the (π,d) or (d,π^*) CT or (d,d) state would participate in the energy relaxation process of photoexcited Cr^{III} porphyrins.

The most prominent changes we observed in the transient Raman spectra of XCr^{III}TPP in THF solvent are the relatively large downshifts of the ν_2 and ν_4 bands, which are sensitive to the core size of the porphyrin ring [Figure 2(a) versus Figure 2(c)]. In this case, the five-coordinate Cr^{III}TPP(THF) structure seems to still be preserved in the excited state, as evidenced by the opposite Raman frequency shift to that of the four-coordinate Cr^{III}TPP* [Figure 1(c)]. Thus, the relative large downshifts of the ν_2 and ν_4 modes observed in the transient Cr^{III}TPP(THF)* species are mainly induced by the electronic state of this transient species. The similar changes in the transient Raman spectra were also observed for XCr^{III}TPP in pyridine solvent. Although the involvement of (d,d) and (π,d_π) CT states in the deactivation processes of photoexcited Cr^{III} porphyrins has not been clarified to date, Gouterman et al.[9,17] and Harriman[16] suggested that the low-lying spin forbidden (d,d) transition may contribute to the nonradiative decay from the emissive $^4T_1(\pi,\pi^*)$ excited state (Figure 7B). However, the intrametal (d,d) electronic transition is considered to have little effect on the electronic structure of the porphyrin ring macrocycle. Although the energies of $d_{x^2-y^2}$ and d_{z^2} orbitals involved in the (d,d) transitions are influenced by the presence of axial ligands, such as THF and pyridine, the main deactivation channel of photoexcited Cr^{III} porphyrins in benzene is different from that in THF and pyridine. Judging from a large downshift of some transient Raman modes and a significant reduction of the lifetime of photoexcited Cr^{III} porphyrins in THF (632 ps in THF versus ~1 ms in benzene), the electronic nature of the low-lying quenching state below the normally emissive tripmultiplet (π,π^*) excited states in Cr^{III}TPP(THF)* is likely to possess (π,d) or (d,π^*) CT character. The downshift of ~10 cm^{-1} in the ν_2 and ν_4 modes for Cr^{III}TPP(THF)* is roughly in parallel with the frequency shift of the same Raman bands in the formation of the porphyrin π-cation radical. In concordance with these discussions, the electronic transition from the HOMO porphyrin ring (π) orbital to the singly occupied d_π orbital to form the (π,d_π) CT state seems to be the most plausible process for the formation of the low-lying quenching state of the normally emissive tripmultiplet (π,π^*) excited states (Figure 7A). Therefore, we can suggest that (π,d_π) CT transition is responsible for the main deactivation channel after photoexcitation of Cr^{III} porphyrins in THF (Figure 7B). On the other hand, Zwaans et al.[25] reported the theoretical prediction that the Cr—N distance in neutral ClCr^{III}TPP is shorter than that in anionic ClCr^{III}TPP, which possesses highly charged Cr^{III} ion for the accommodation of extra charge. These results indicate that the core sizes of the

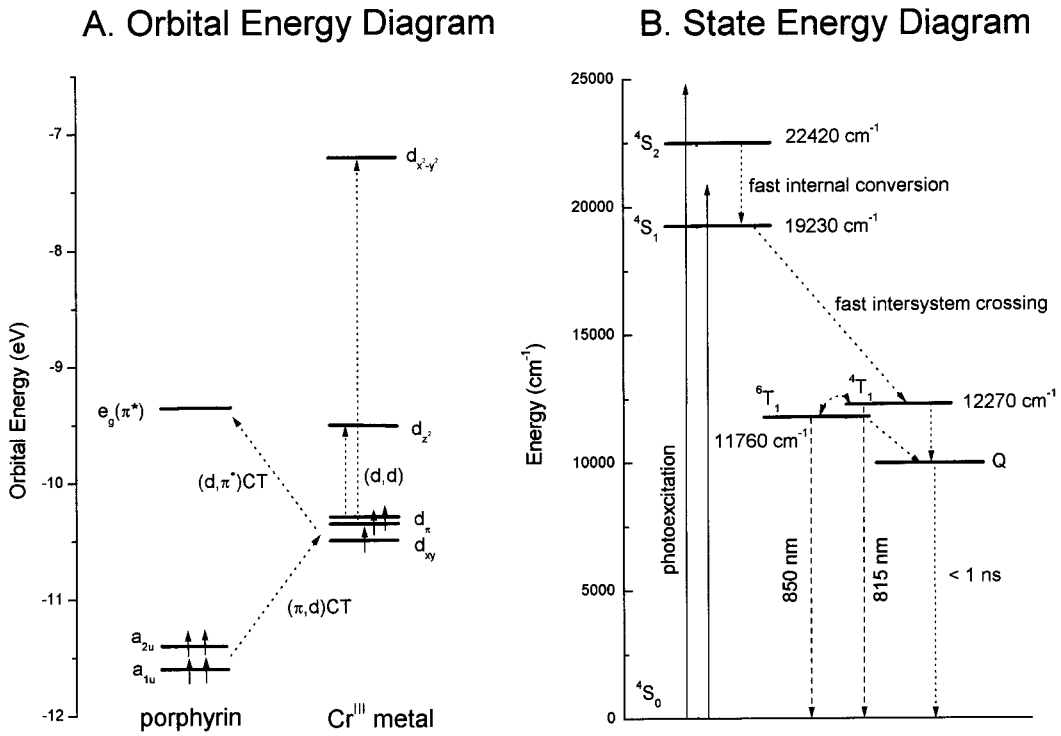

Figure 7. (A) Top-filled and the lowest empty orbital energies by the IEH model. (B) Proposed energy-level diagram for $ClCr^{III}TPP$ in THF. The locations of the electronic states in this scheme are from the previous luminescence investigation of $ClCr^{III}TPP$ and our measurements. The location of the proposed quenching [Q, (π,d_π) CT] state is dependent on the solvents employed.

porphyrin macrocycles are affected by the charge in the central metal ion. Thus, considering the increased core size in the excited state, the deactivation state is expected to be the (π,d_π) CT transition accompanied by an increase in metal ion charge.

As for the photodissociation of the sixth-ligand in Cr^{III} porphyrins, Yamaji et al.[15] reported that the $^4S(\pi,\pi^*)$ state is responsible for the photodissociation process of $ClCr^{III}TPP(py)$. However, it is unlikely that the porphyrin ring (π,π^*) state is a dissociative channel for the axial ligand because the axial ligand interacts mainly with the d orbitals of Cr^{III} metal. Hence, if the transient absorption as well as the transient resonance Raman spectrum originates from the proposed (π,d) CT state, an increase in the electron density in the d_π orbital with a z-axis component should induce a repulsive interaction between the Cr^{III} metal and axial ligand on photoexcitation. This change in electron density of the metal d orbital then gives rise to an efficient photodissociation process of axial halogen ligands if the Cr^{III} porphyrin has a six- or five-coordinate structure (Figure 7A).

5. Conclusions

The axial ligand photodissociation processes of $XCr^{III}TPP$ (X = Cl or Br) have been investigated in various solvents by transient Raman and absorption spectroscopic techniques. In benzene, the upshift of the ν_2 and ν_4 bands and the disappearance of Cr—X stretching mode in the transient Raman spectra indicate the photodissociation of axial ligand halogen atoms in the excited state. The temporal evolutions of photoinduced absorption and bleaching signals of $XCr^{III}TPP$ in benzene exhibit biphasic decay profiles, with time constants of 1 and 20 ms. The fast decay is attributed to the four-coordinate photoexcited $Cr^{III}TPP^*$ species, and the relatively slow decay component seems to be due to the recombination process returning to the original five-coordinate $XCr^{III}TPP$ species. In THF, however, the transient spectroscopic data indicate that the axial ligand halogen atoms photodissociate to form the five-coordinate Cr^{III}-TPP(THF) species on photoexcitation. A significant reduction in the lifetimes of photoexcited $ClCr^{III}TPP$ in THF was observed as compared with that in benzene. This behavior is believed to arise from the five-coordinate transient $Cr^{III}TPP(THF)^*$ species, which decays with a time constant of 632 ps due to the participation of low-energy states in the deactivation process. The electronic nature of the lowest excited state of the five-coordinate $Cr^{III}TPP(THF)^*$ species is suggested to possess a (π,d_π) CT character based on the comparison of transient Raman and absorption spectral features with those of other paramagnetic metalloporphyrins.

Acknowledgment. This work was supported by the National Creative Initiatives Research Program of the Ministry of Science and Technology of Science (D.K.) and by the Basic Science Research Institute Program, the Ministry of Education (BSRI-98-3432) (M.Y.).

Supporting Information Available: Figures showing Raman and absorption spectra of $ClCr^{III}TPP$. This information is available free of charge via the Internet at http://pubs.acs.org.

References and Notes

(1) Hoshino, M.; Hirai, T. *J. Phys. Chem.* **1987**, *91*, 4510.
(2) Harriman, A.; Porter, G.; Richoux, M. C. *J. Chem. Soc., Faraday Trans. 2* **1981**, *77*, 833.
(3) Seely, G. R. *Photochem. Photobiol.* **1978**, *27*, 639.
(4) Leondiadis, L.; Momenteau, M.; desbois, A. *Inorg. Chem.* **1992**, *31*, 461.
(5) Han, S.; Rousseau, D. L.; Giacometti, G.; Brunori, M. *Proc. Natl. Acad. Sci. U.S.A.* **1990**, *87*, 205.
(6) Coletta, M.; Ascenzi, P.; Brunori, M. *J. Biol. Chem.* **1988**, *258*, 473.
(7) Alder, R. G.; Chavez, M. D.; Ondrias, M. R.; Courtney, S. H.; Friedman J. M. *J. Am. Chem. Soc.* **1990**, *112*, 3241.
(8) Petrich, J. W.; Poyart, C.; Martin, J. L. *Biochemistry.* **1988**, *27*, 4049.
(9) Gouterman, M. In Porphyrins; Dolphin, D.; Ed.; Academic: New York, 1978; Vol. III, Chapter 1.

(10) (a) Yamaji, M.; Hama, Y.; Miyazaki, Y.; Hoshino, M. *Inorg. Chem.* **1992**, *31*, 932. (b) Fleisher, E. B.; Krishnamurthy, M. *J. Am. Chem. Soc*. **1971**, *93*, 3784.

(11) Summerville, D. A.; Jones, R. D.; Hoffman, B. M.; Basolo, F. *J. Am. Chem. Soc*. **1977**, *99*, 8195.

(12) Hoshino, M.; Nagamori, T.; Seki, H.; Chihara, T.; Tase, T.; Wakatsuki, Y.; Inamo, M. *J. Phys. Chem*. **1998**, *102*, 1297.

(13) Hoshino, M.; Tezuka, N.; Inamo, M. *J. Phys. Chem*. **1996**, *100*, 627.

(14) Inamo, M.; Hoshino, M.; Nakajima, K.; Aizawa, S.; Funabashi, S. *Bull. Chem. Soc. Jpn*. **1995**, *68*, 2293.

(15) Yamaji, M.; Hama, Y.; Hoshino, M. *Chem. Phys. Lett*. **1990**, *165*, 309.

(16) Harriman, A. *J. Chem. Soc., Faraday Trans. 1* **1982**, *78*, 2727.

(17) Gouterman, M.; Hanson, L. K.; Khalil, G.-E.; Leenstra, W. R.; Buchler, J. W. *J. Chem. Phys.* **1975**, *62*, 2343.

(18) Jeoung, S. C.; Kim, D.; Cho, D. W.; Yoon, M.; Ahn, K.-H. *J. Phys. Chem.* **1996**, *100*, 8867.

(19) Jeoung, S. C.; Kim, D.; Cho, D. W.; Yoon, M. *J. Phys. Chem.* **1996**, *100*, 3075.

(20) Parthasarathi, N.; Hansen, C.; Yamaguchi, S.; Spiro, T. G. *J. Am. Chem. Soc*. **1987**, *109*, 3865.

(21) Kashiwagi. H.; Obara, S. *Int. J. Quantum Chem.* **1981**, *20*, 843.

(22) Sekino, H.; Kobayashi, H. *J. Chem. Phys.* **1981**, *75*, 3477.

(23) Bell, S. E. J.; Al-Obaidi, A. H. R.; Hegarty, M. J. N.; McGarvey, J. J.; Hester, R. E. *J. Phys. Chem*. **1995**, *99*, 3959.

(24) Sato, S.; Kitagawa, T. *Appl. Phys. B*, **1994**, *59*, 415.

(25) Zwaans, R.; van Lenthe, J. H.; den Boer, D. H. W. *J. Mol. Struct. Theochem*. **1995**, *339*, 153.

(26) Inamo, M.; K. Nakajima. *Bull. Chem. Soc. Jpn*. **1998**, *71*, 883.

(27) Jeoung, S. C.; Kim, D.; Cho, D. W.; Yoon, M. *J. Phys. Chem*. **1995,** *99*, 5826.

(28) Kim, D.; Holten. D.; Gouterman, M. *J. Am. Chem. Soc.* **1984**, *106*, 2793.